

COBEM-2017-2916

NUMERICAL SIMULATION OF THE FLOW OF SUSPENDED SOFT-CAPSULES THROUGH CONSTRICTED CHANNELS

Jose F. Roca R.

Ivan F.M. Menezes

Marcio S. Carvalho

Department of Mechanical Engineering, Pontifícia Universidade Católica do Rio de Janeiro, Rua Marquês de São Vicente, 225 Gávea, Rio de Janeiro, RJ 22453-900, Brazil

jroca@lmmp.mec.puc-rio.br, ivan@puc-rio.br, msc@lmmp.mec.puc-rio.br

Abstract. *Soft-capsules dispersed in aqueous phase flowing through constricted micro-channels poses an interesting problem presented in a myriad of applications from enhance oil recovery (EOR) methods to flow of red blood cells on hemodynamics. Understanding of dynamics at micro-scale is central to assess the macroscopic flow behaviour in EOR applications. We study the flow in a micro-channel with a constriction, which is a model of a pore-throat connecting two adjacent pore-bodies. Flow of capsules through such geometry defines a fluid-structure interaction problem. A coupled finite element method with immersed boundary method was used to solve the transient problem of a single capsule flowing through a constricted channel. The objective is to determine the pressure drop as a function of flow conditions, capsule geometry, fluid and capsule mechanical properties, i.e. elastic modulus E . Results show that pressure at the inner phase is larger than the outer phase in order to balance the capsule stress. Additionally, an extra pressure is observed when the capsule flows through the constriction. The intensity of this peak varies with capsule size and material properties.*

Keywords: *fluid-structure interaction problem, immersed boundary method, finite element method.*

1. INTRODUCTION

Flow of suspended soft-capsules involves interaction between an incompressible viscous fluid and an elastic membrane. This type of configuration finds applications in different scenarios such hemodynamics, specifically flow of red blood cells (Hu *et al.*, 2014), suspension of particles flowing in porous media, among others. Further details may be found in Barthès-Biesel (2016).

Membrane dynamics in viscous flow defines a fluid-structure interaction problem (FSI). In the literature, there are different methods to address them; they usually need high computation requirements to solve fluid-solid dynamics equations on adaptable or evolving grids. Immersed boundary method (IBM) developed by Peskin (1972) has been explored in the present study. His objective was to study flow patterns around heart valves by modelling flexible characteristics of muscle fibers. Thus, this method is capable to describe membrane dynamics treated as a flexible boundary immersed in a fluid domain.

IBM utilizes an Eulerian/Lagrangian description, where a flexible capsule, hereafter *the structure* is transported by flow dynamics (Peskin and McQueen, 1989). In this approach, the structure is considered as a part of fluid domain where additional forces are exerted. A Lagrangian variable describes the position of the immersed boundary with respect to a fixed coordinate system. The interaction of the structure on the fluid is considered as an external force in the incompressible Navier-Stokes equations, whilst points describing the structure are advected by fluid velocity field.

Mathematically, the external force is a singular vector field, zero everywhere except around the structure; therefore, conveniently defined by Dirac delta function. Peskin (1972) utilized a finite difference approximation for Dirac delta function. However, since finite element method (FEM) has been used here, there is no need for such approximation, only evaluate its effect through weighting functions as reported by Boffi and Gastaldi (2007).

2. MATHEMATICAL DESCRIPTION

The problem of flow of a flexible structure through a constricted channel is addressed by simplifying the capsule surface as a $1D$ massless structure referenced in a $2D$ Cartesian coordinate system XY .

Figure 1 depicts the flow domain described by an Eulerian reference system. The flexible structure (red) is composed by discrete points defining a Lagrangian frame.

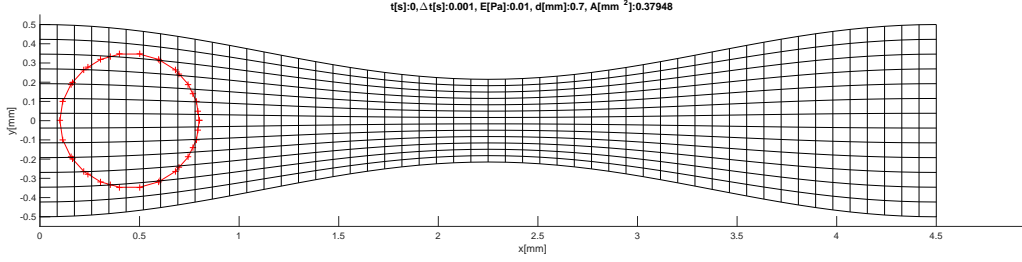


Figure 1. Sketch of flow domain.

For an incompressible viscous fluid, mass and momentum conservation equations in an Eulerian frame are defined as

$$\begin{aligned}\bar{\nabla} \cdot \bar{u} &= 0, \\ \rho \frac{\partial \bar{u}}{\partial t} + \rho \bar{u} \cdot \bar{\nabla} \bar{u} &= \bar{\nabla} \cdot \bar{\tau} + \bar{F}^B,\end{aligned}\quad (1)$$

where ρ , $\bar{u} = [u, v]$, $\bar{\tau}$ and \bar{F}^B are density, velocity vector field, stress tensor field and body force, respectively.

Considering incompressible Newtonian fluid, stress tensor $\bar{\tau}$ is defined as

$$\bar{\tau} = -p\bar{I} + \mu[\bar{\nabla}\bar{u} + (\bar{\nabla}\bar{u})^T], \quad (2)$$

where p and μ represent pressure and absolute viscosity, respectively.

As mentioned before, interaction between the structure and the fluid is computed through a source term in momentum equation, and represented by an integral along the surface Γ

$$\bar{F}^B = \int_{\Gamma} \bar{f} \delta(\bar{x} - \bar{X}(s_1, s_2, r, t)) ds_1, \quad (3)$$

where \bar{x} , $\bar{X}(s_1, s_2, r, t)$ and δ are independent variable in Eulerian frame, position of structure in Lagrangian frame and Dirac delta function, respectively. However, since the structure is a transient $1D$ model, $\bar{X} = \bar{X}(s_1, t)$.

Therefore, \bar{f} defined as a force density, is applied to the fluid as follows

$$\bar{f} = \frac{\partial(T\bar{t})}{\partial s_1}, \quad (4)$$

where \bar{t} is the unit tangent vector along s_1 direction, and T is the structure tension.

Furthermore, since the elastic structure obeys Hooke's law, for a stressed configuration, tension T depends linearly on the distance of two nearby points at any time and the distance of the same points in a reference configuration. Therefore, T can be written as

$$T = E \left| \frac{\partial \bar{X}}{\partial s_{10}} \right|, \quad (5)$$

where E is the modulus of elasticity of the material, and s_{10} defines the arc length along s_1 at the reference configuration.

Additionally, the points of the structure are advected by the velocity, due to no-slip condition.

$$\frac{\partial \bar{X}}{\partial t} = \bar{u}(\bar{X}(s_1, t), t) \quad (6)$$

2.1 Boundary and initial conditions

At the initial time $t = 0$ s, all fields, velocity and pressure, are equal zero, and the structure is initially centered at $x = 0.45$ mm, as was shown in Fig. 1.

A parabolic velocity profile was imposed at the inlet

$$\begin{aligned} u(x=0, y) &= \frac{3V(t)}{2} \left[1 - \left(\frac{2y}{H} \right)^2 \right], \\ v(x=0, y) &= 0, \end{aligned} \quad (7)$$

where $V(t)$ is the transient average velocity of the continuous phase, and H is the entrance distance between the upper and lower surfaces. At the outflow, a fully developed flow and zero pressure $p_{(x=L)} = p_{out} = 0$ Pa are considered as follows

$$\bar{n} \cdot \bar{\nabla} \bar{u}|_{x=L} = \bar{0}, \quad (8)$$

where \bar{n} is the outward normal vector and L is the geometry length.

Furthermore, no-slip/no-penetration condition is assumed at the upper and lower walls:

$$\bar{u} = \bar{0}. \quad (9)$$

Regarding the numerical scheme, the finite element method has been used to solve momentum and continuity equations. Time discretization utilized predictor-corrector algorithm and Newton's method addressed nonlinearities. The resultant algebraic system was LU factorized using MATLAB[®] solver.

As already mentioned, an additional force term in the Navier-Stokes equations was included in residuals of elements near the structure. Finally, the position of Lagrangian points is explicitly estimated with the updated velocity field.

3. RESULTS AND DISCUSSION

The objective is to determine the pressure drop $\Delta p = p_{in} - p_{out}$ along the constricted channel for different structure properties.

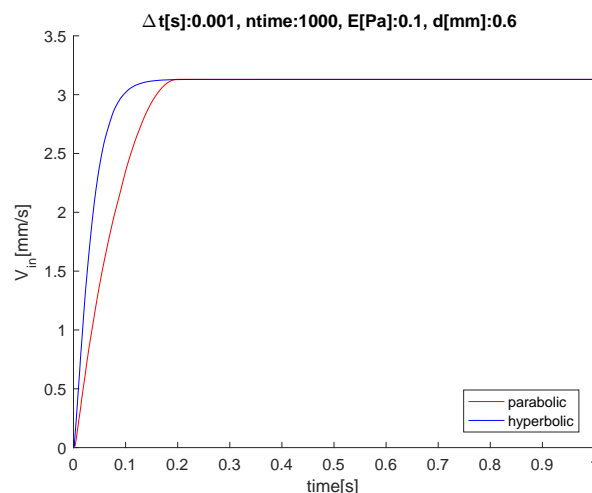


Figure 2. Two different centerline velocity functions at $x = 0$.

Throughout this work, a single geometry was analyzed. The entrance distance between the upper and lower surfaces H is 1 mm, constriction ratio $\alpha = 0.43$ and the total length $L = 4.5$ mm. We used 13×52 quadrangular elements, and the number of initial points describing the structure ranged from 20 to 25. Additionally, structures of different diameters d and elastic modulus E were tested. Regarding fluid properties, a fluid similar to water, $\rho = 1000$ kg/m³ and $\mu = 0.001$ Pa.s, was utilized for inner and outer phases.

The centerline velocity V_{in} at $x = 0$ reaches smoothly steady-state conditions after 20% of simulation time. Figure 2 shows the two different functions used: a parabolic function and the hyperbolic function \tanh . Notice that the hyperbolic function reaches steady-state conditions sooner than the parabolic function, and that such behaviour will impact transient response of pressure drop.

Although transient response of pressure drop is a function of the profiles tested (hyperbolic response is faster than parabolic one), the additional pressure needed to have the structure deformed through the constriction has been slightly affected, as indicated by the similarity between peaks in Fig. 3.

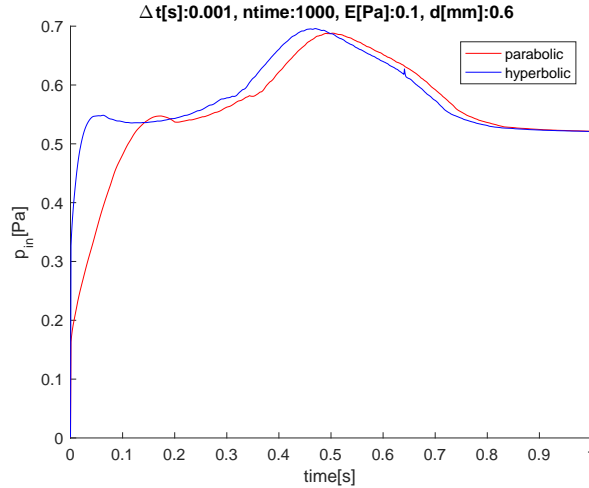


Figure 3. Pressure drop response in time for different V_{in} .

In order to analyze pressure drop under different conditions, some cases are defined in Table 1. For a given channel of constant width, all cases run under the same flowrate per unit width $q = 2.0845 \text{ mm}^2/\text{s}$, which corresponds to the Reynolds number, $Re \approx 2$.

Table 1. Cases tested for different E and d .

$d[\text{mm}] \setminus E[\text{Pa}]$	0.01	0.1
0.6	C1	C2
0.7	C4	C5

Time evolution of a particular case C4 is shown in Fig. 4. It should be pointed out that, structure in red is marked for reference purposes only. Note that the structure is continuously refined. In fact, the final number of Lagrangian points is far greater at the end of simulation. The basic idea is to avoid any absence of Lagrangian points when a linear segment of the structure crosses an element.

Inlet velocity increases from zero to the steady-state value during $t = 0.2 \text{ s}$. Notice a parabolic profile at the inlet. Additionally, velocity vectors are larger in the constriction region due to change in the geometry, and consequent fluid acceleration. Regarding pressure field distribution, which is zero referenced at the outlet, pressure inside the structure is larger than outer pressure throughout simulation. This pressure difference balances structure stresses. Moreover, injection pressure (or pressure drop) increases in order to get the structure deformed through the constriction, as already discussed in Fig. 3. After that, nonetheless, pressure decreases monotonically to values related to flow without structure. In the selected case, C4, the maximum injection pressure occurs at $t = 0.365 \text{ s}$, as indicated in Fig. 4(c). In fact, the determination of the maximum pressure is of paramount importance to this study.

After the constriction, although the structure starts to recover its original form, loss of fluid contained inside the structure is observed. Figure 5 summarizes this behavior for the different cases. Observe that this issue gets worse when the elastic modulus increases (C2 and C5). Currently, this problem is being addressed and some improvements are under test, i.e. refining Eulerian mesh may help to a certain extent.

As already stated, flowrate conditions and fluid properties remain unaltered, in order to correctly assess the effect of

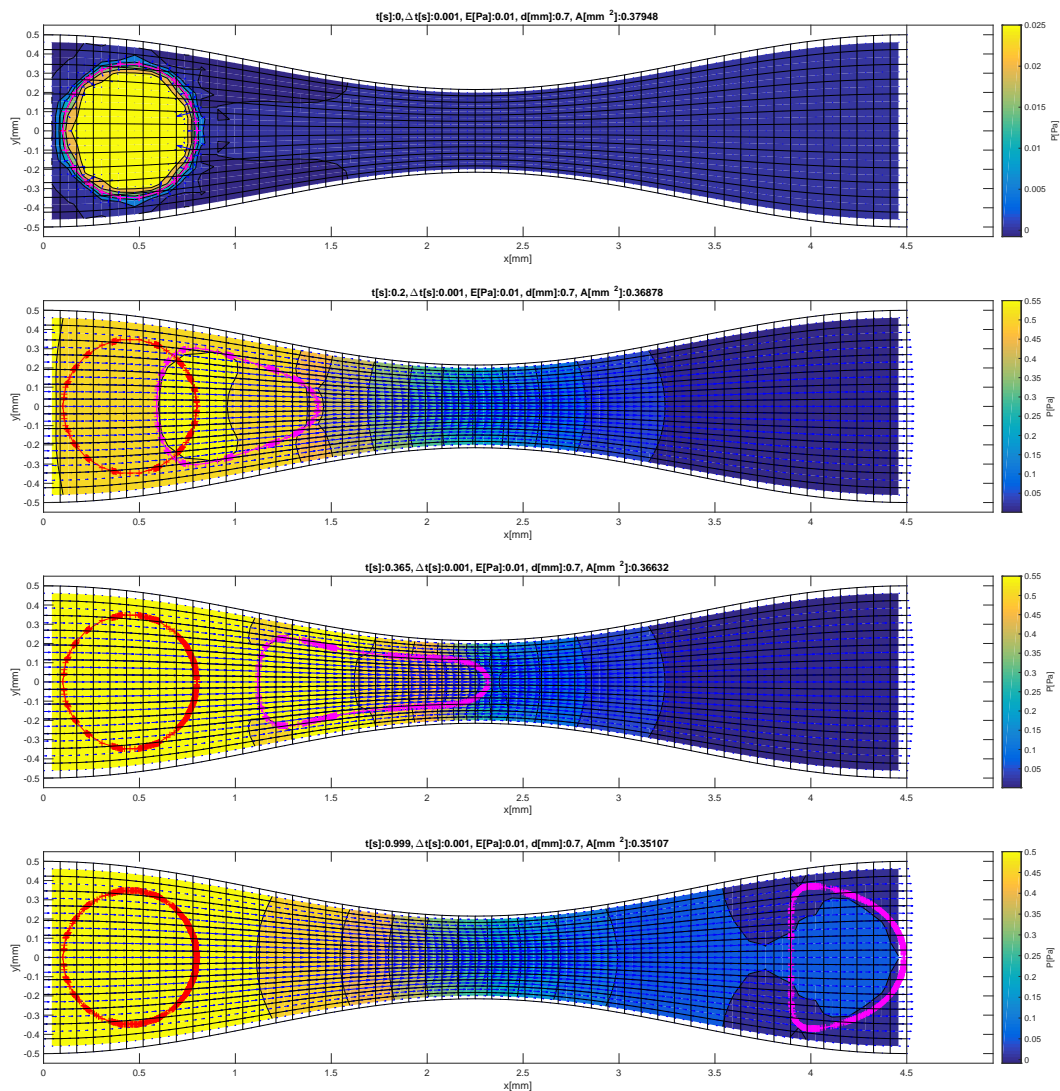


Figure 4. Velocity and pressure fields for case C4 as time evolves: (a) $t = 0$ s, (b) $t = 0.2$ s, (c) $t = 0.365$ s and (d) $t = 0.999$ s.

structure size d and elastic modulus E on pressure response, as illustrated in Fig. 6. Note that all curves present a small overshoot related to the transient response of increasing flowrate, even the flow without structure. On the other hand, the

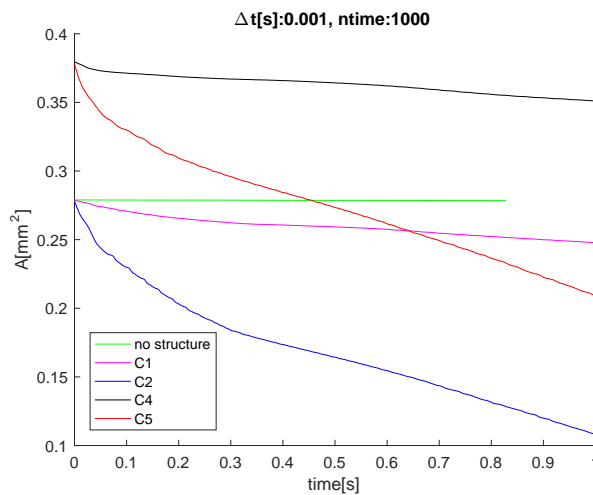


Figure 5. Loss of fluid contained inside the structure for different cases.

second peak refers to the extra pressure needed to get the structure through the constriction. It is observed that, the larger elastic modulus E , the larger the extra pressure. In addition, given an elastic material, the larger structure d , the larger pressure peak. Finally, after the constriction, pressure fairly returns to its steady-value.

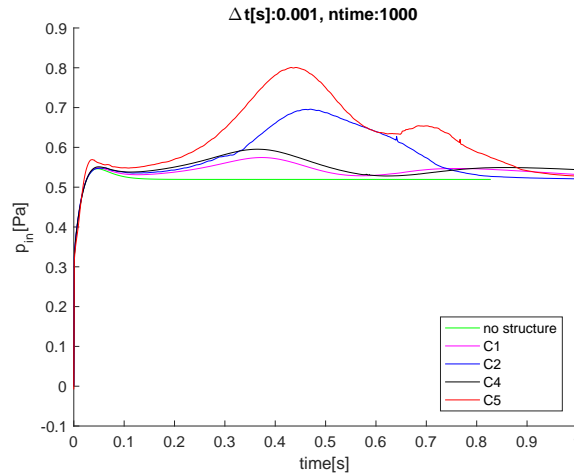


Figure 6. Pressure drop response in time for different cases.

4. FINAL REMARKS

The flow of a soft-capsule through a constricted channel has been studied by an Eulerian/Lagrangian approach utilizing finite element coupled with immersed boundary methods. Such methodology considers the effect of the 1D structure on fluid dynamics by the source term in the Navier-Stokes equations.

Results show that transient of the centerline velocity has minimal effect in the extra pressure needed to have the structure deformed through the constriction. In fact, this extra pressure is a function of the structure diameter d and the elastic modulus E . For a given material, the larger the structure, the larger the extra pressure. Additionally, for a given structure size, the *stiffer* the material, the larger the extra pressure.

Elastic modulus has an important effect on loss of fluid inside the structure. This issue is currently under investigation.

5. ACKNOWLEDGEMENTS

This work was carried out in association with the ongoing project registered as *Escoamento de dispersões complexas em meios porosos heterogêneos: análise na escala de poro e macroscópica (PUC-Rio/BG Brasil/Shell Brasil/ANP)* – Complex Dispersion Flow Through Porous Media – funded by BG Brasil/Shell Brasil under the ANP R&D levy as *Compromisso de Investimentos com Pesquisa e Desenvolvimento*.

6. REFERENCES

- Barthès-Biesel, D., 2016. “Motion and deformation of elastic capsules and vesicles in flow”. *Annual Review of Fluid Mechanics*, Vol. 48, No. 1, pp. 25–52.
- Boffi, D. and Gastaldi, L., 2007. “The immersed boundary method: a finite element approach”. *Computational Fluid and Solid Mechanics*, Vol. 7, No. 2-4, pp. 230–236.
- Hu, W., Kim, Y. and Lai, M., 2014. “An immersed boundary method for simulating the dynamics of three-dimensional axisymmetric vesicles in navier-stokes flows”. *Journal of Computational Physics*, Vol. 257.
- Peskin, C., 1972. “Flow patterns around heart valves: A numerical method”. *Journal of Computational Physics*, Vol. 10.
- Peskin, C. and McQueen, D., 1989. “A three-dimensional computational method for blood flow in heart i. immersed elastic fibers in a viscous incompressible fluid”. *Journal of Computational Physics*, Vol. 81.

7. RESPONSIBILITY NOTICE

The authors are the only responsible for the printed material included in this paper.